systematic studies of beam-normal single spin asymmetries at MAMI

Michaela Thiel
on behalf of the A1 collaboration
Institut für Kernphysik, Johannes Gutenberg-Universität Mainz

JG|U

elastic electron scattering

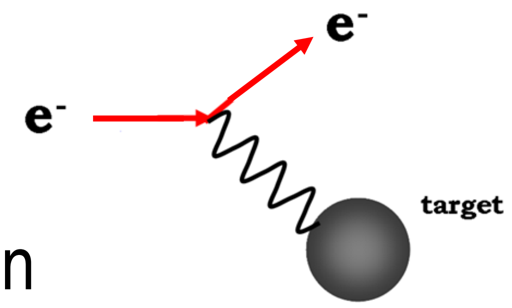

high-precision experiments ➡ need to go beyond Born approximation

one-photon exchange

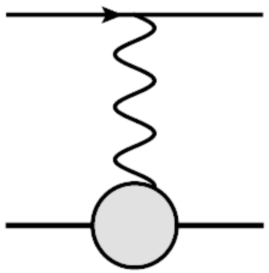

purely real

+

two-photon exchange

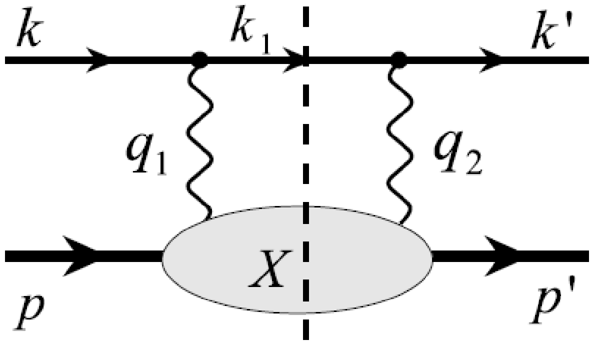

has imaginary part

elastic electron scattering

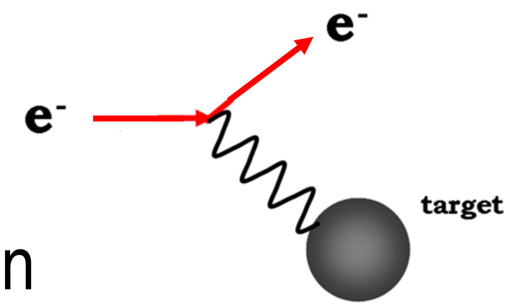

high-precision experiments ➡ need to go beyond Born approximation

one-photon exchange

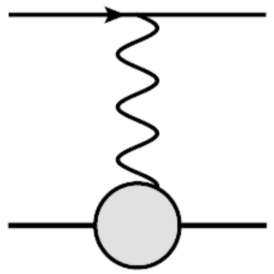

purely real

+

two-photon exchange

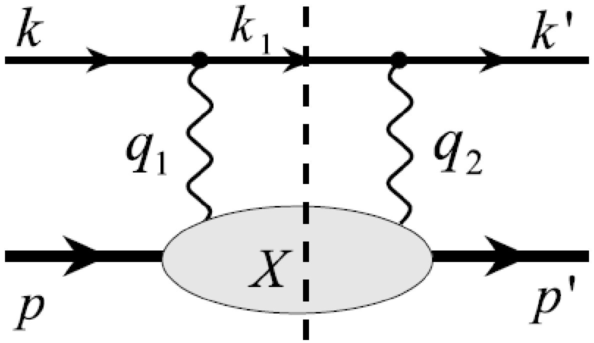

has imaginary part

interference of one- and two-photon exchange causes

beam-normal single spin asymmetry A_n

De Rújula et al., Nucl. Phys. B35, 365 (1971)

➡ **allows access of imaginary part of 2γ exchange amplitude**

theoretical treatment of A_n

consider contributions of elastic (scales as Z)
AND inelastic intermediate states (scales as A/Z)

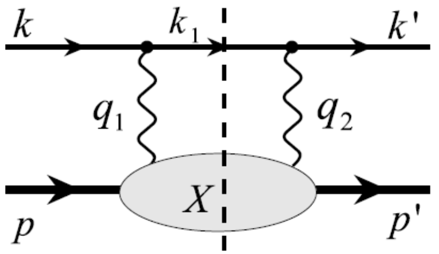

dispersion integral over intermediate excited states

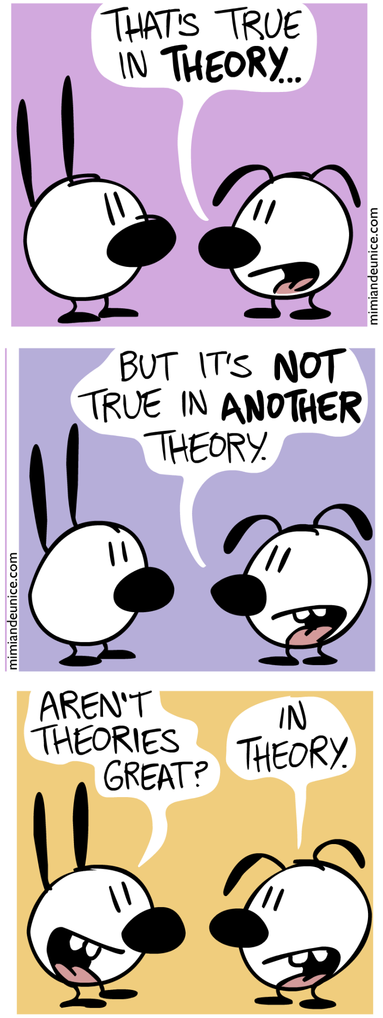

theoretical treatment of A_n

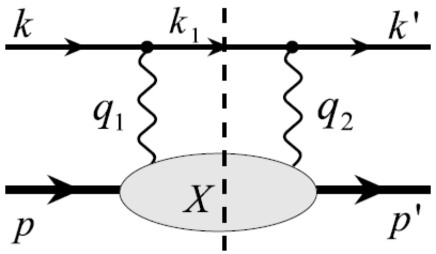

consider contributions of elastic (scales as Z)
AND inelastic intermediate states (scales as A/Z)

dispersion integral over intermediate excited states

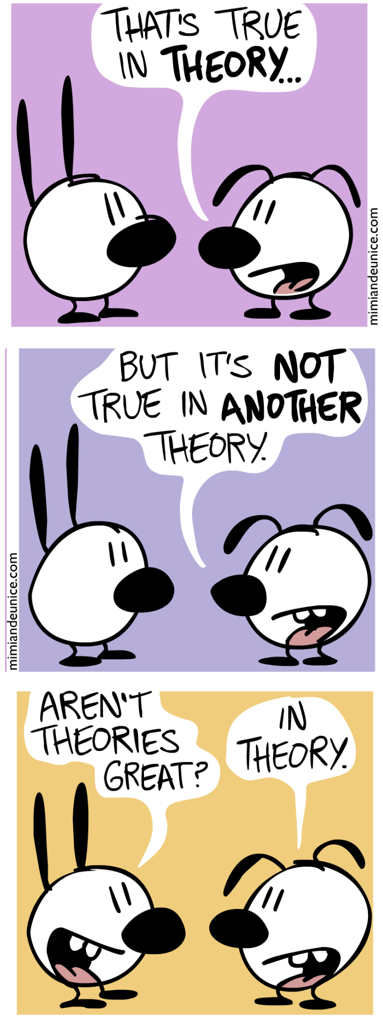

focus on very low four-momentum transfer:

leading order $\sim C_0 \cdot \log\left(\frac{Q^2}{m^2}\right) \cdot \frac{F_{Compton}(Q^2)}{F_{ch}(Q^2)}$

C_0 contains energy dependence

can be calculated exactly!

Gorchtein and Horowitz, Phys. Rev. C77, 044606 (2008)

experimental access to A_n

elastic electron-nucleus scattering + NEW e⁻ polarization: vertical

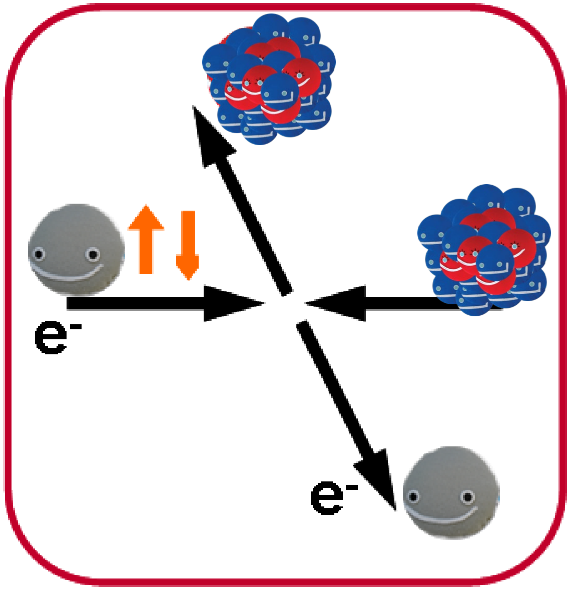

experimental access to A_n

elastic electron-nucleus scattering + NEW e^- polarization: vertical

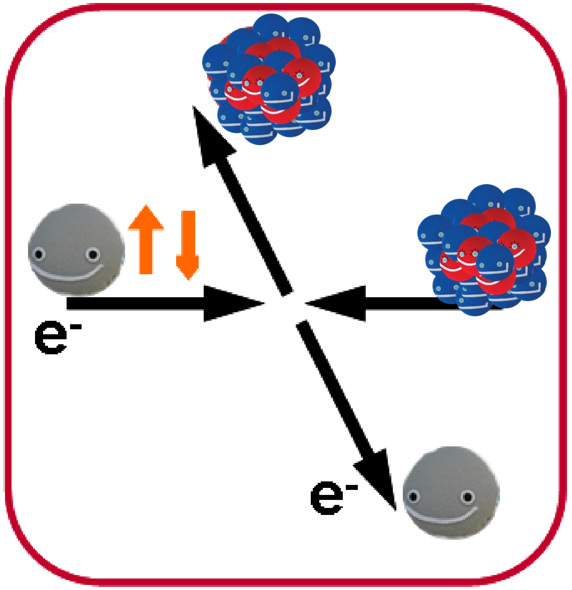

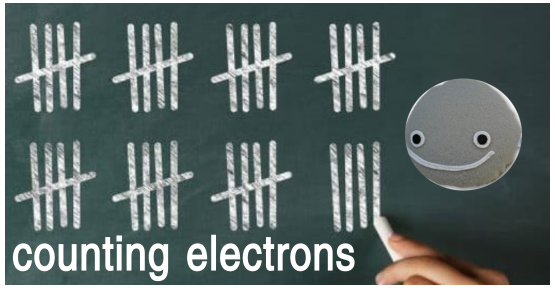

$$A_n = \frac{\sigma^\uparrow - \sigma^\downarrow}{\sigma^\uparrow + \sigma^\downarrow} \approx 10^{-6} - 10^{-5}$$

experimental access to A_n

elastic electron-nucleus scattering + NEW e⁻ polarization: vertical

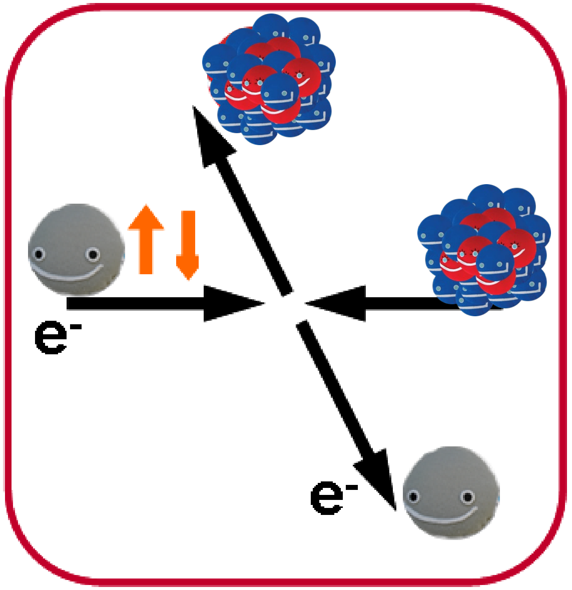

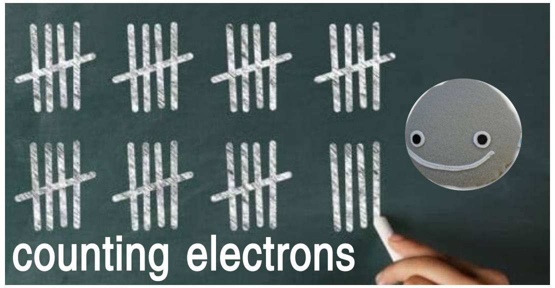

$$A_n = \frac{\sigma^{\uparrow} - \sigma^{\downarrow}}{\sigma^{\uparrow} + \sigma^{\downarrow}} \approx 10^{-6} - 10^{-5}$$

- improve knowledge of TPE effects + benchmark theoretical models
- can cause false asymmetry in high-precision parity-violating electron scattering experiments (neutron skin, weak charge of the proton)

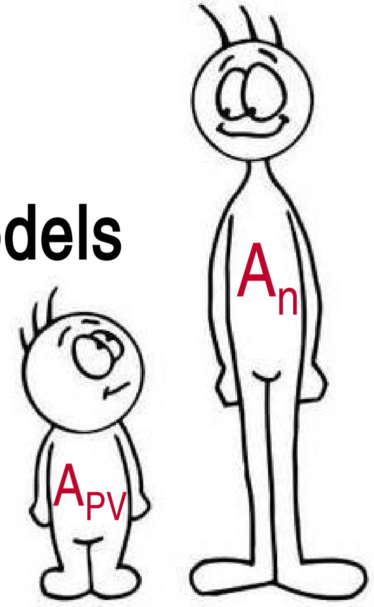

how it all started

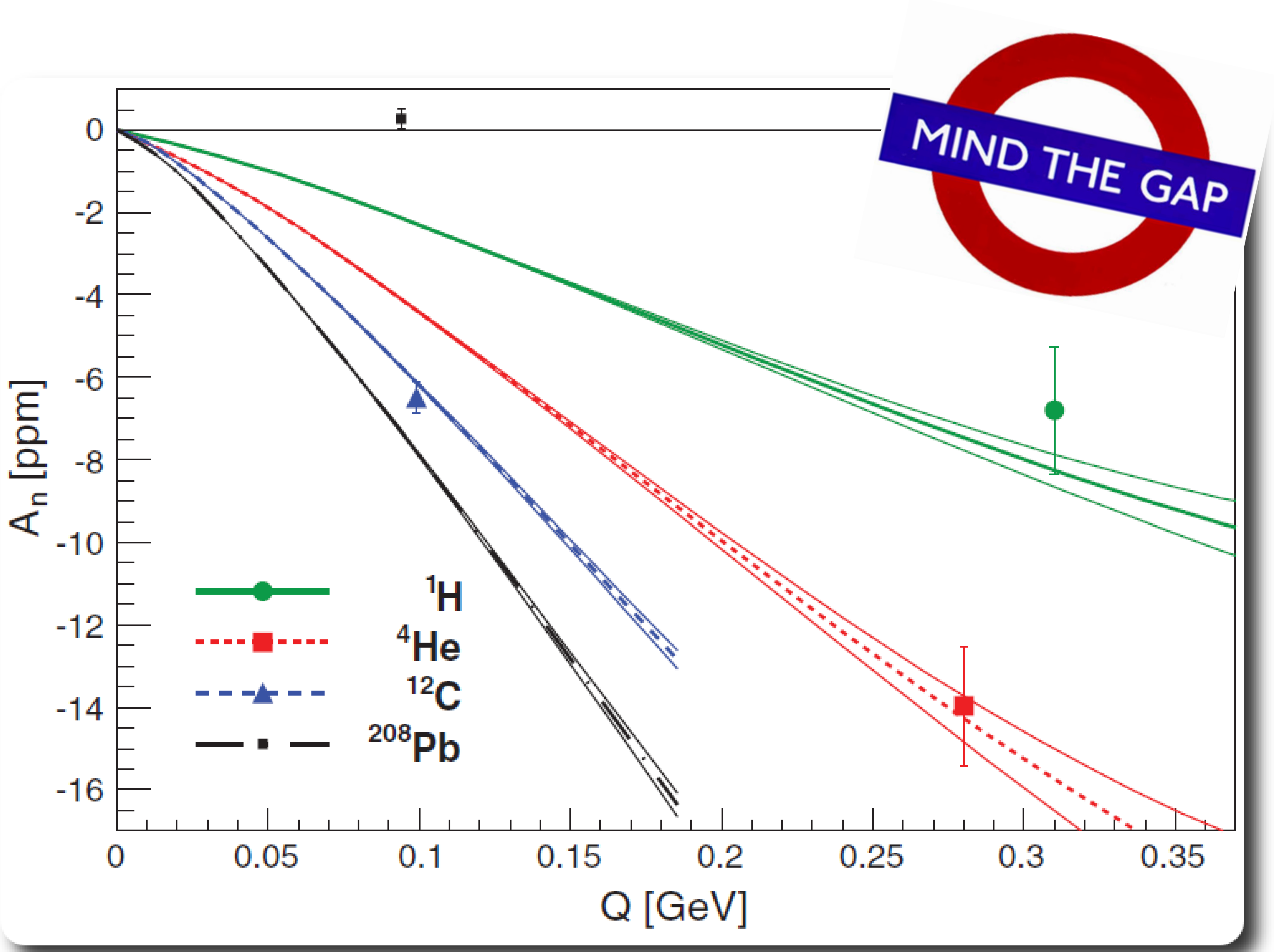

S. Abrahamyan et al., PRL 109, 192501 (2012)

the whole nuclear chart in a small band

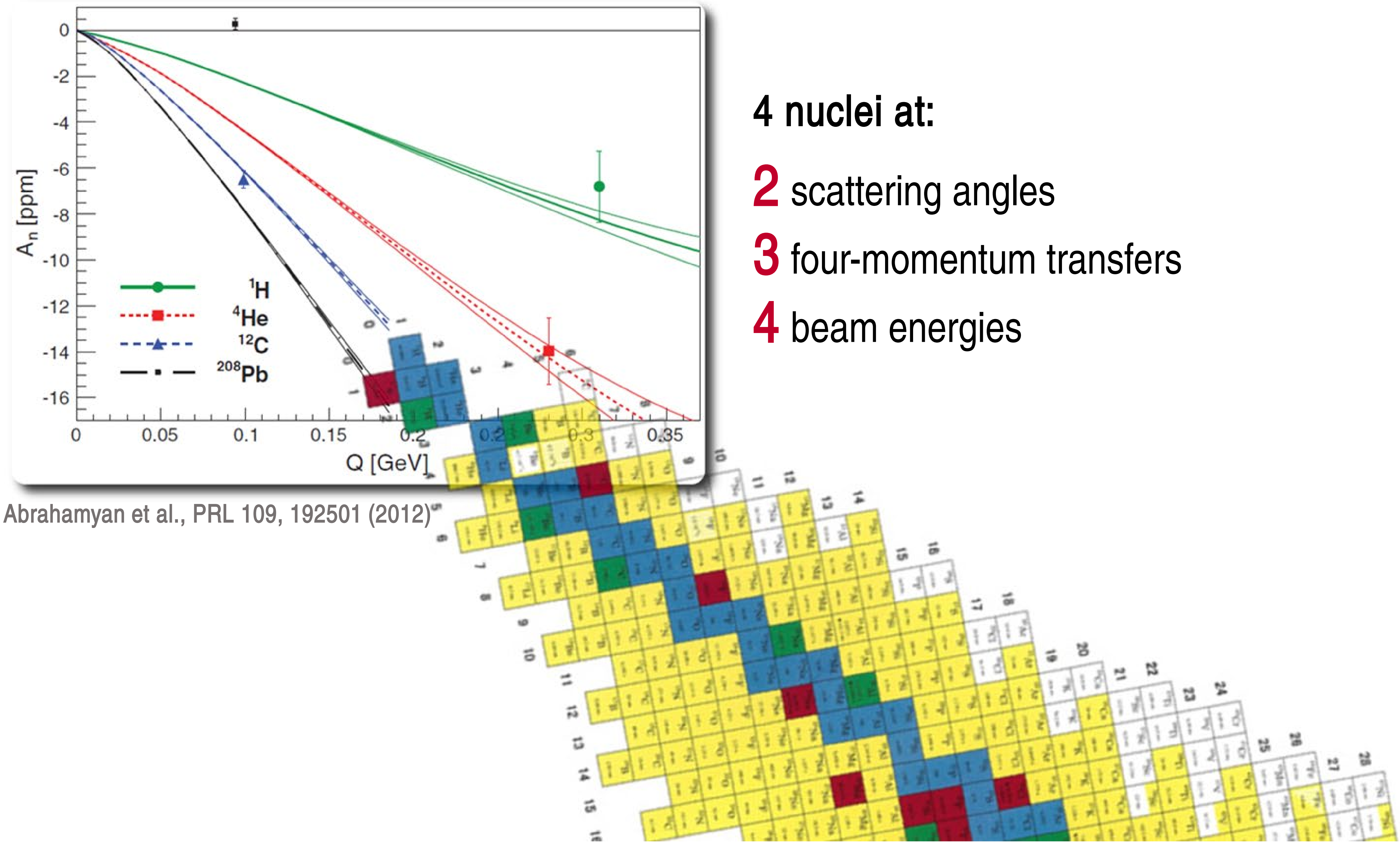

S. Abrahamyan et al., PRL 109, 192501 (2012)

4 nuclei at:

2 scattering angles

3 four-momentum transfers

4 beam energies

the whole nuclear chart in a small band

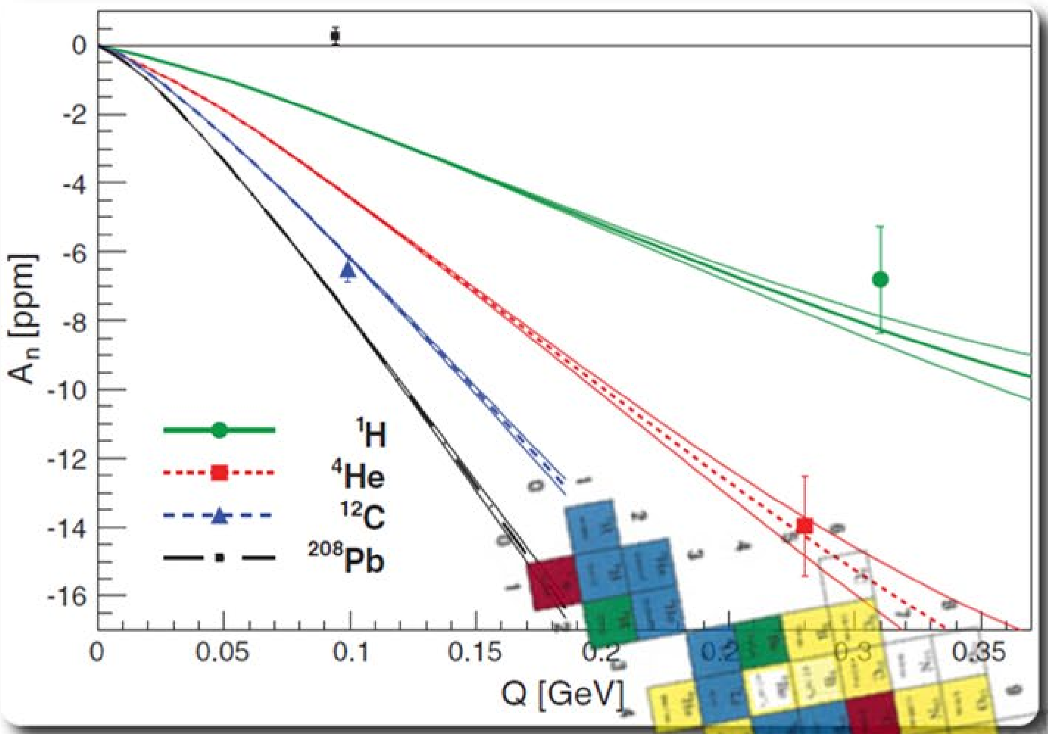

S. Abrahamyan et al., PRL 109, 192501 (2012)

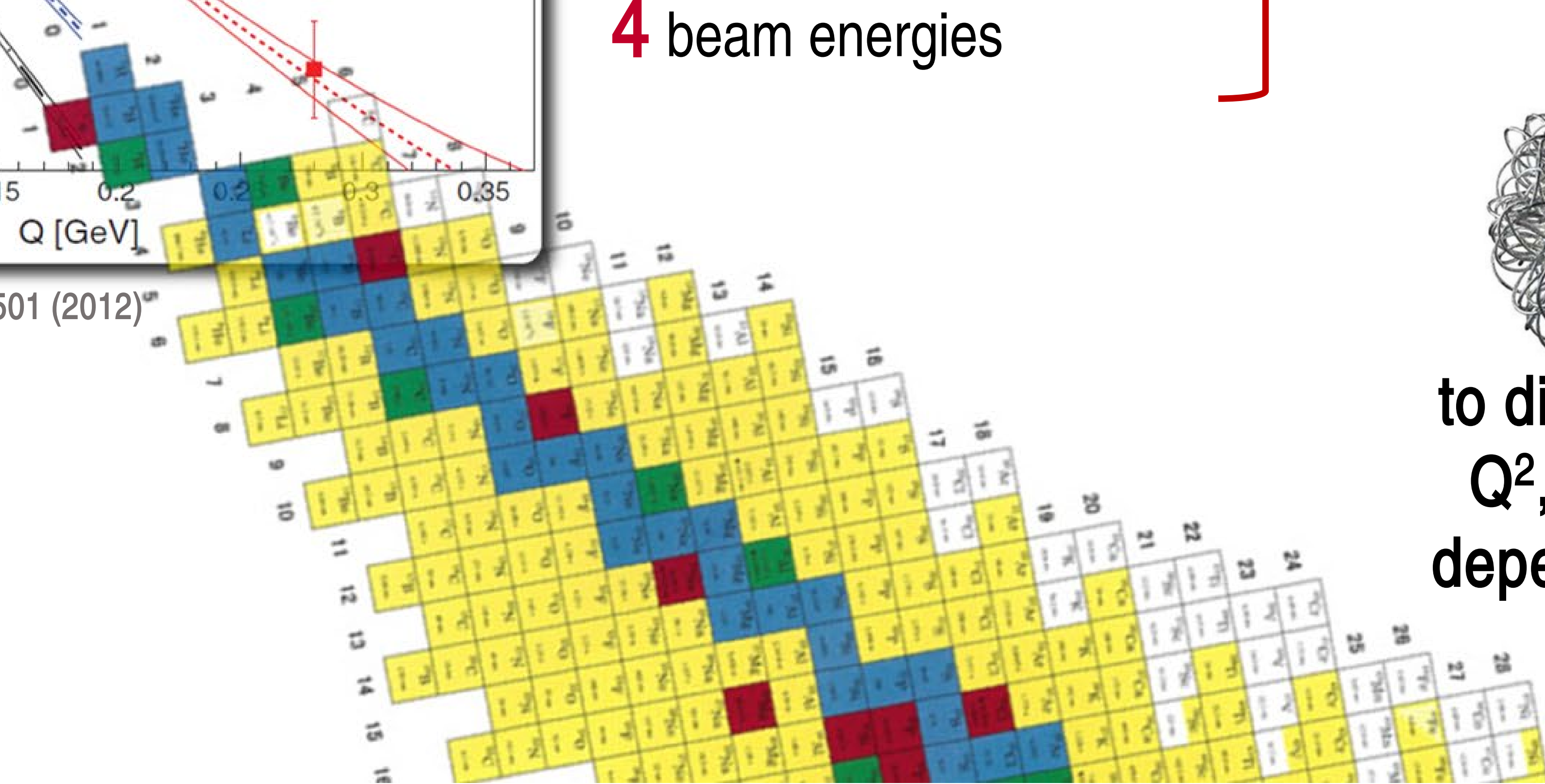

4 nuclei at:

2 scattering angles

3 four-momentum transfers

4 beam energies

systematic study needed

to disentangle Q^2, Z and E dependencies!

the stage

MAinz MIcrotron (MAMI)

up to E = 1.6 GeV

resolution

$\sigma_E < 0.1$ MeV

reliability

85% (7000 h/a)

polarization

up to 80% @ 40μA

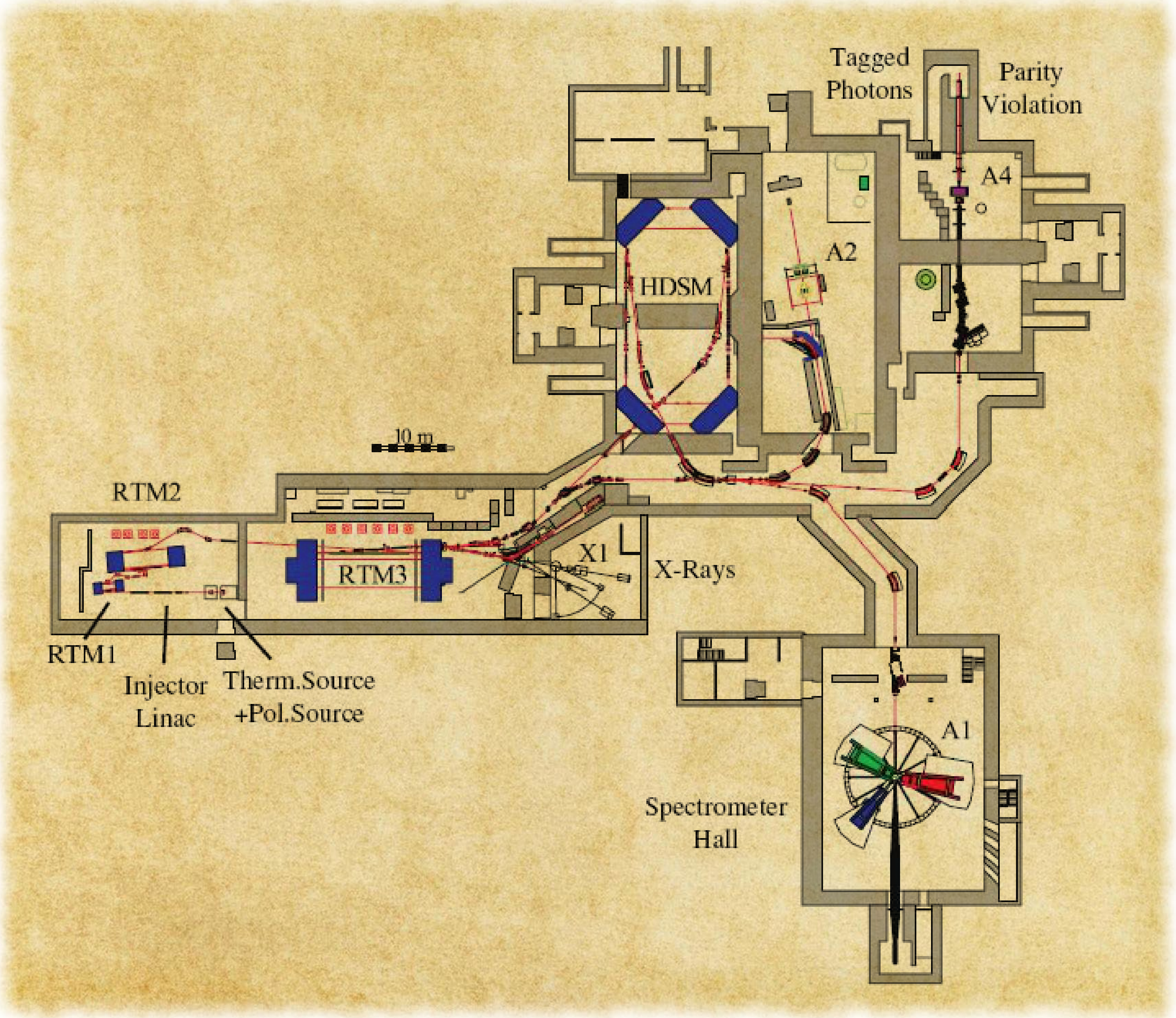

polarimetry measure vertical transverse polarization

THE TOOLS:

Mott: horizontal transverse @ source

Møller: longitudinal @ target

polarimetry measure vertical transverse polarization

THE TOOLS:

Mott: horizontal transverse @ source

Møller: longitudinal @ target

polarimetry measure vertical transverse polarization

THE TOOLS:

Mott: horizontal transverse @ source

Møller: longitudinal @ target

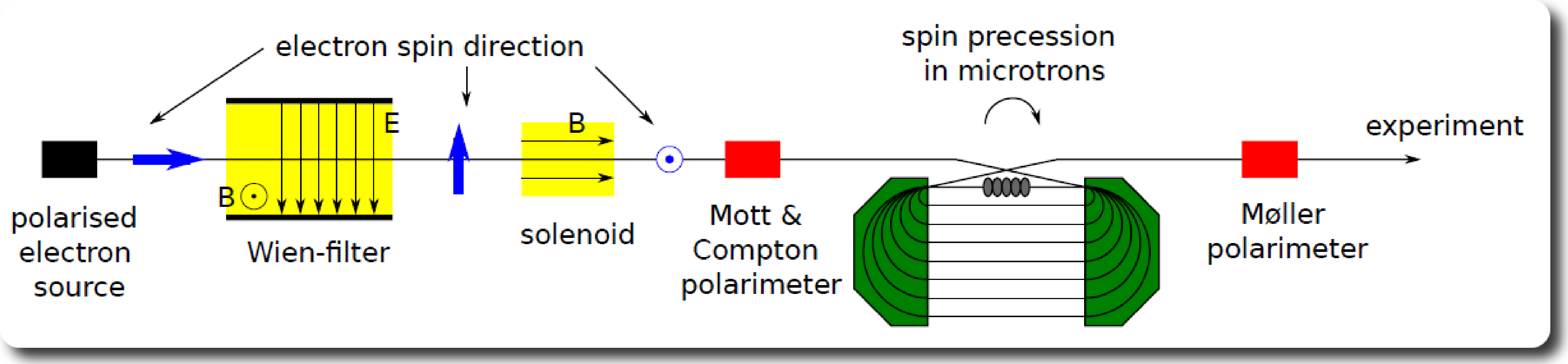

B.S. Schlimme et al., Nucl. Instrum. Meth. A 850, 54 (2017)

THE METHOD:

MAXIMIZE longitudinal polarization @ target

MAXIMIZE horizontal transverse component @ source

MINIMIZE longitudinal and transverse component @ source and target

experimental setup

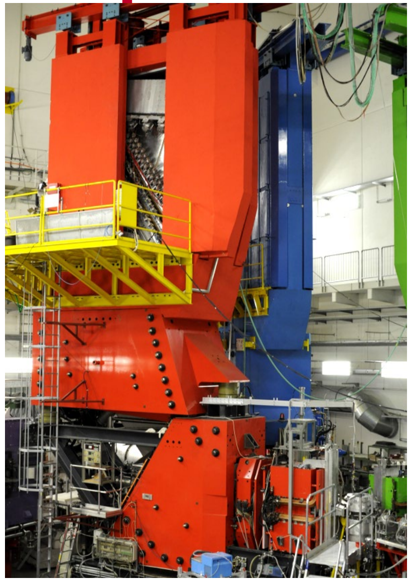

magnetic
spectrometer

+

fused-silica Cherenkov detectors

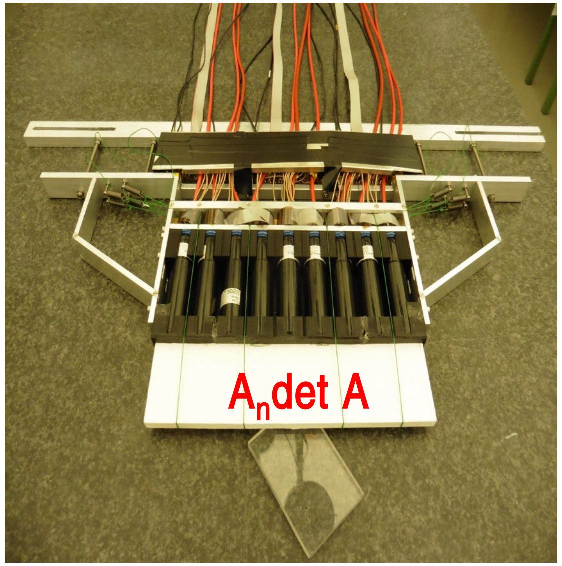

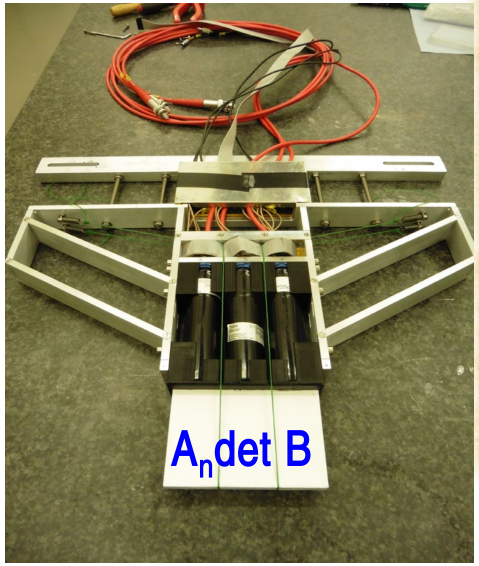

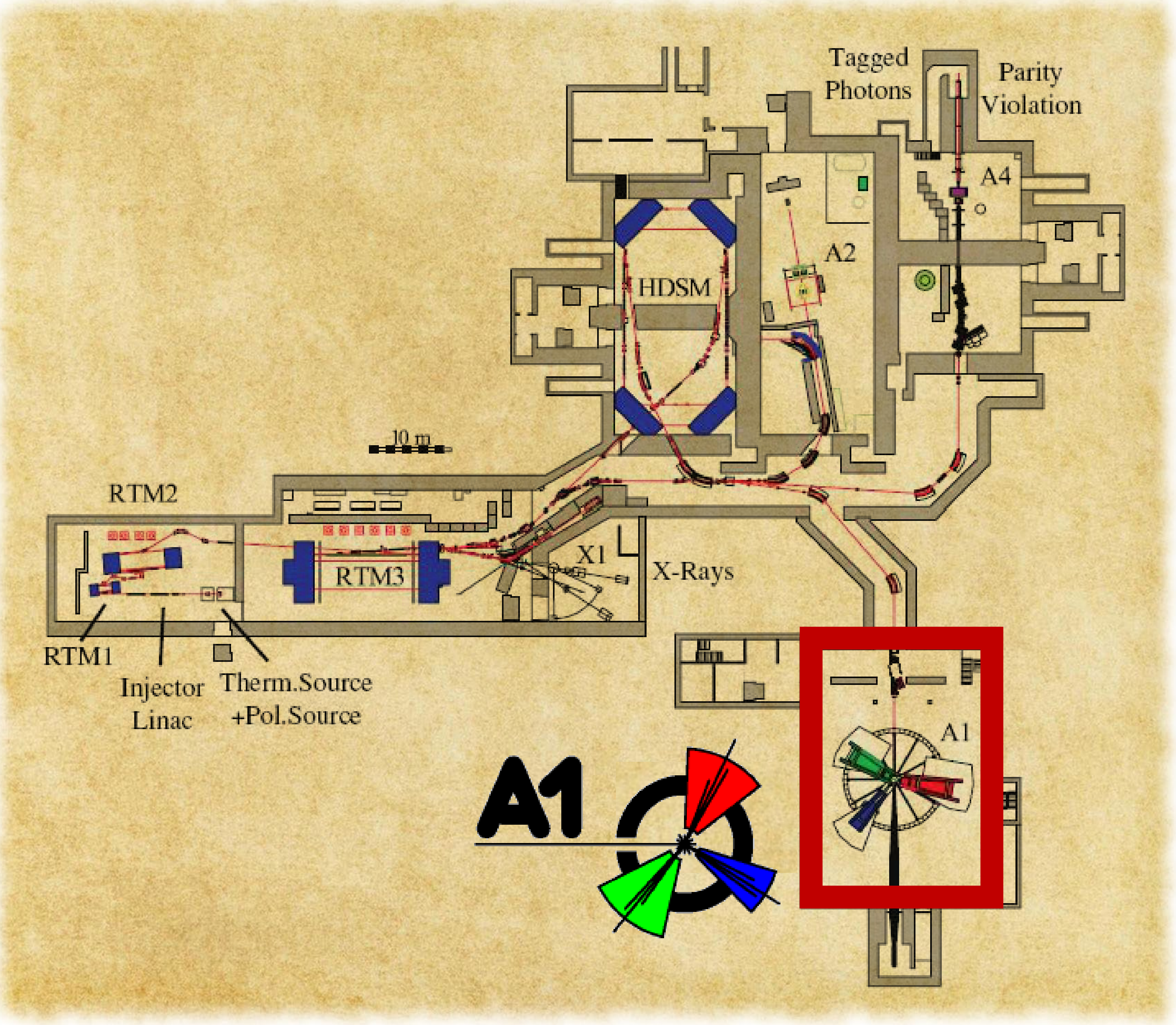

spectrometer mode

precise positioning of detectors

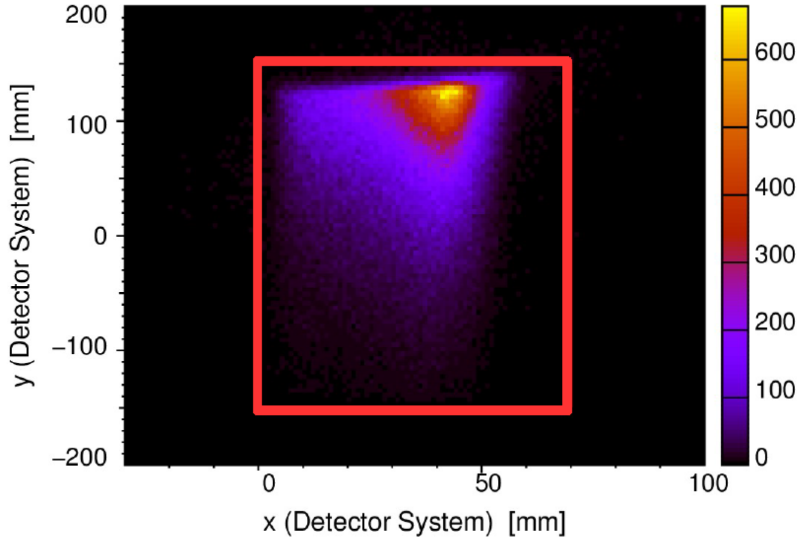

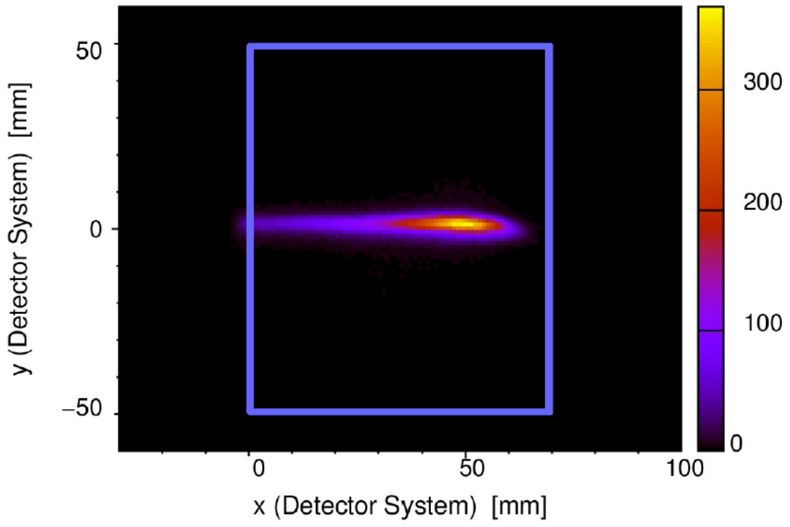

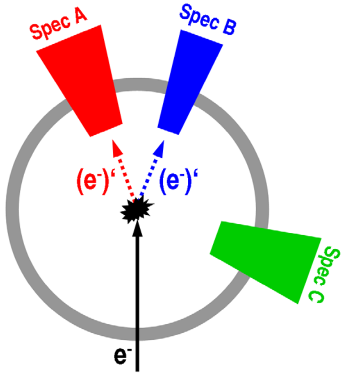

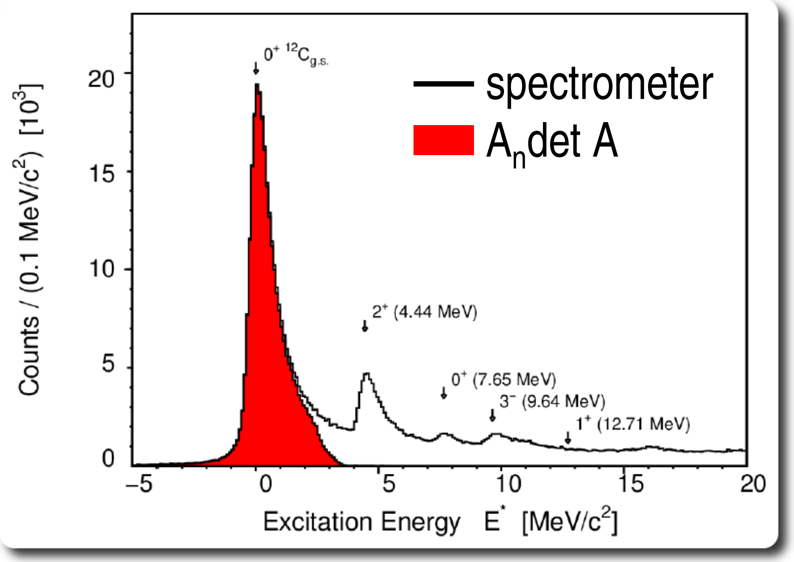

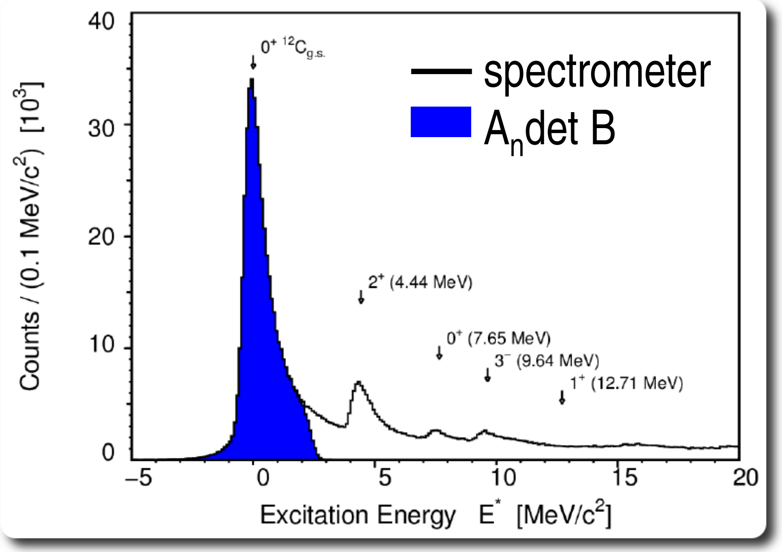

instrumental asymmetries

beam related sources:

current

energy

position and angle

stabilization system needed!

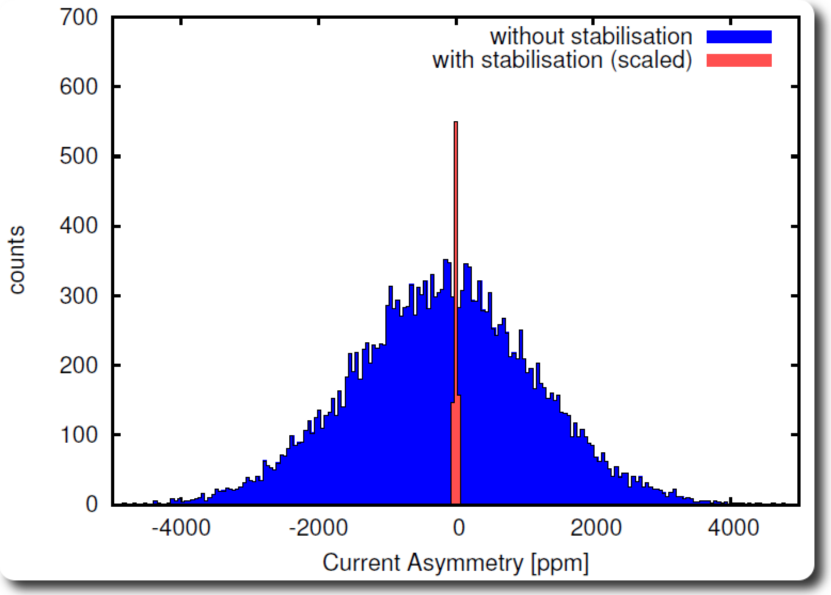

instrumental asymmetries

beam related sources:
current
energy
position and angle

stabilization system needed!

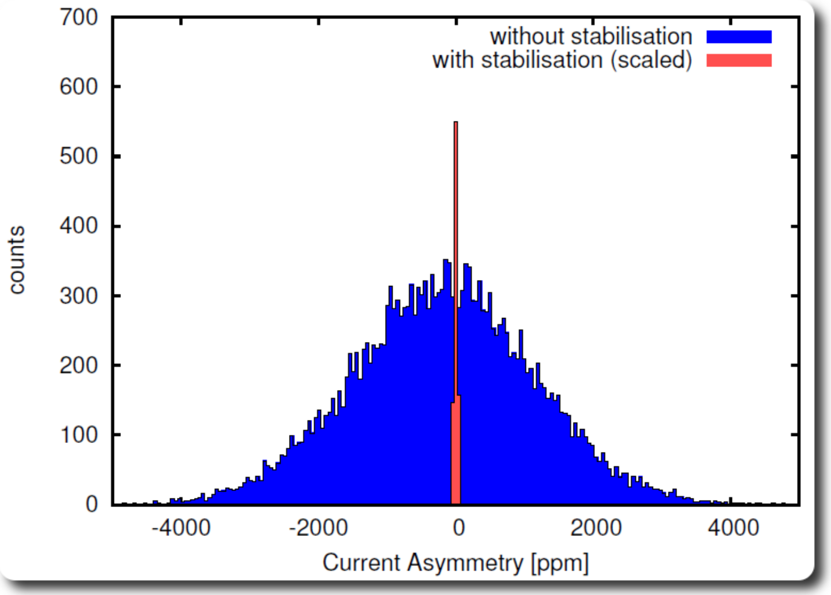

non-beam related sources:
ground noise
gate length fluctuations
electrical cross talk

hardware suppression:

$\otimes \odot \odot \otimes \quad \odot \otimes \otimes \odot$

synchronization with power grid
random polarity sequence
inversion of general sign

results – Q² dependence

$0.02\ \mathrm{GeV}^2 \lesssim Q^2 \lesssim 0.05\ \mathrm{GeV}^2$

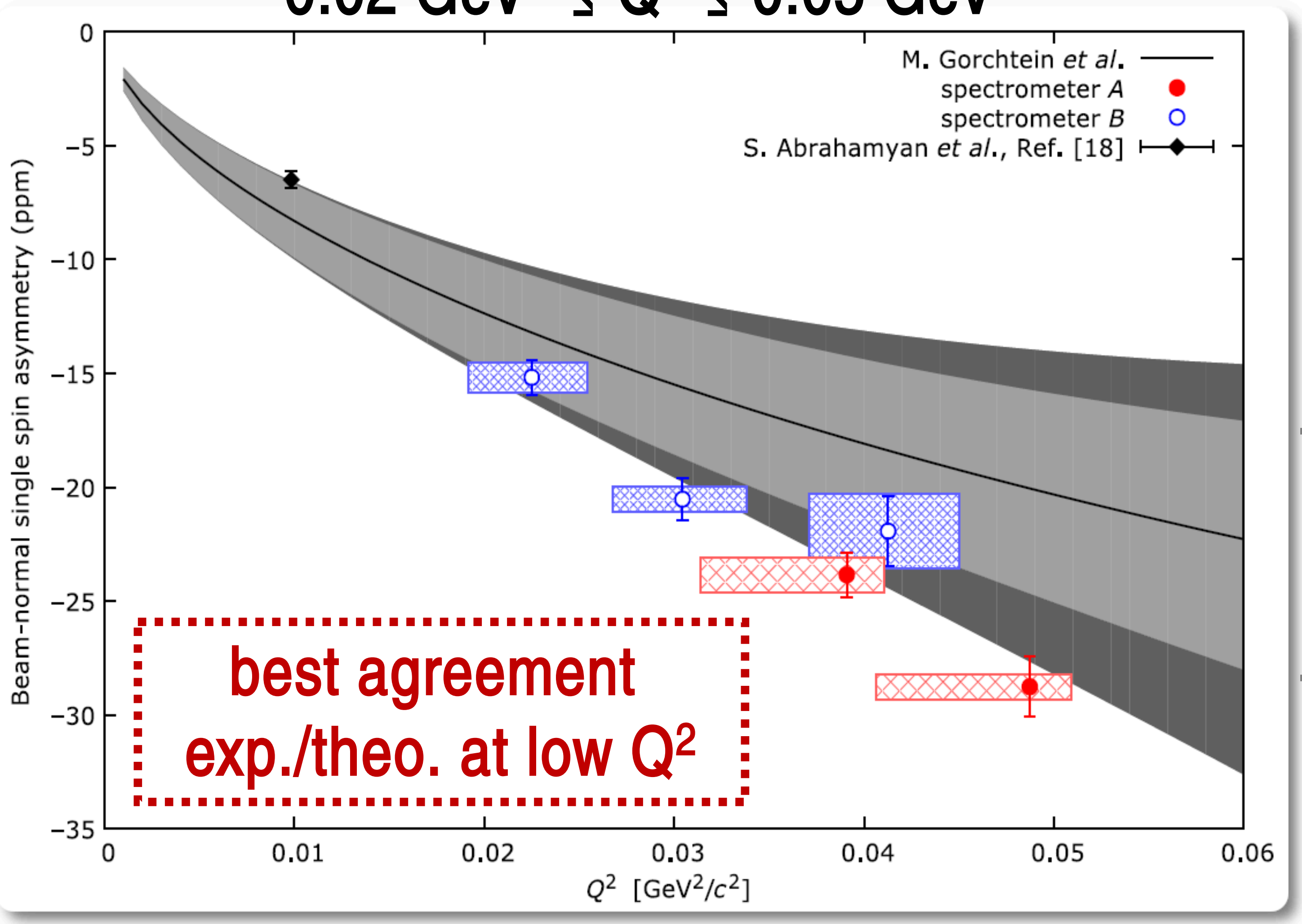

A. Esser et al., PRL 121, 022503 (2018)

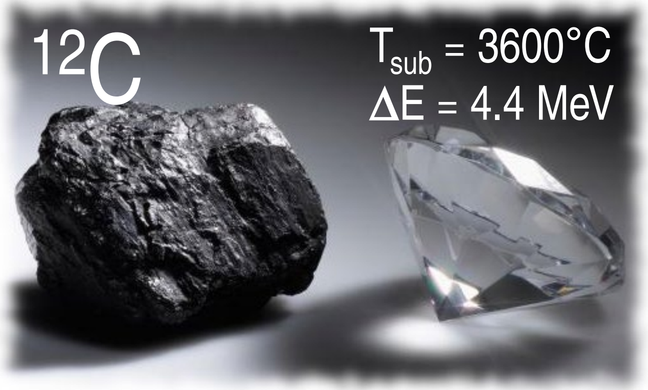

uncertainty of
Compton slope parameter:

± 10%

± 20%

results – A dependence

^{12}C, ^{28}Si, ^{90}Zr (Q^2 = 0.04 GeV^2)

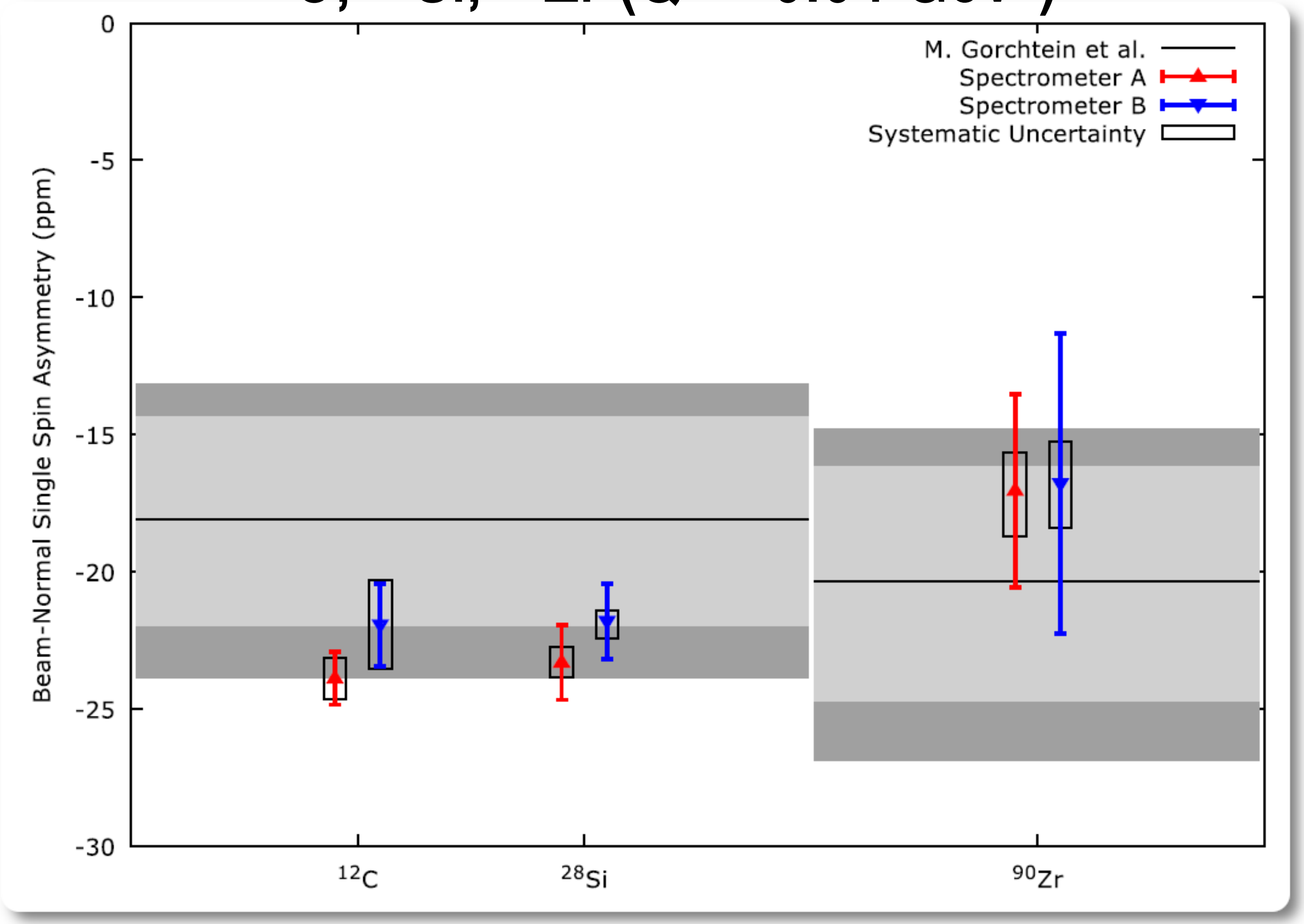

uncertainty of
Compton slope parameter:

± 10%   ± 20%

A. Esser et al., PLB 808, 135664 (2020)

Compton slope parameter

Q^2 dependence reconstructed from differential cross section for Compton scattering

$$\frac{d\sigma}{dq^2} \approx a e^{-B|q^2|} F_{ch}^2(q^2) + \sigma_{inc}$$

Compton slope parameter

Q^2 dependence reconstructed from differential cross section for Compton scattering

$$\frac{d\sigma}{dq^2} \approx a e^{-B|q^2|} F_{ch}^2(q^2) + \sigma_{inc}$$

theory suggested approximate independence of $F_{compton}(Q^2)/F_{ch}(Q^2)$ from the target nucleus due to available high-energy Compton scattering data on ^1H and ^4He
for PRL 121 (022503) 2018 and PLB 808 (135664) 2020

Compton slope parameter

Q^2 dependence reconstructed from differential cross section for Compton scattering

$$\frac{d\sigma}{dq^2} \approx a e^{-B|q^2|} F_{ch}^2(q^2) + \sigma_{inc}$$

theory suggested approximate independence of $F_{compton}(Q^2)/F_{ch}(Q^2)$ from the target nucleus due to available high-energy Compton scattering data on ^{1}H and ^{4}He for PRL 121 (022503) 2018 and PLB 808 (135664) 2020

measurements are available:

- at high energies, E ~ 3–5 GeV
- for the targets ^{4}He, ^{12}C, ^{27}Al, ^{49}Ti, ^{64}Cu, ^{109}Ag, ^{197}Au

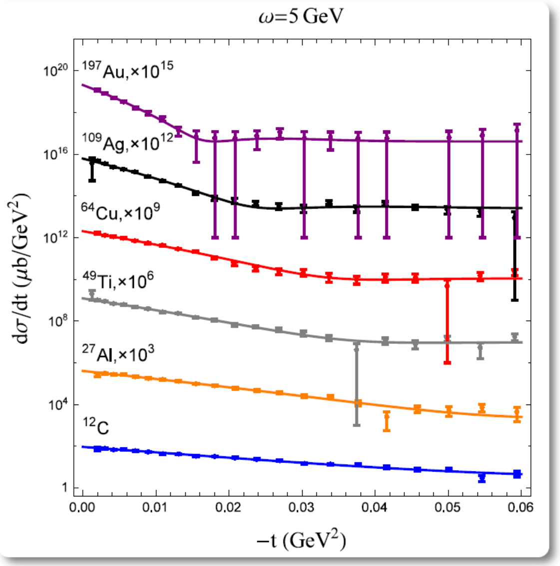

O. Koshchii et al., Phys. Rev. C 103, 064316 (2021)

Compton slope parameter

Q^2 dependence reconstructed from differential cross section for Compton scattering

$$\frac{d\sigma}{dq^2} \approx a e^{-B|q^2|} F_{ch}^2(q^2) + \sigma_{inc}$$

theory suggested approximate independence of $F_{compton}(Q^2)/F_{ch}(Q^2)$ from the target nucleus due to available high-energy Compton scattering data on ^{1}H and ^{4}He for PRL 121 (022503) 2018 and PLB 808 (135664) 2020

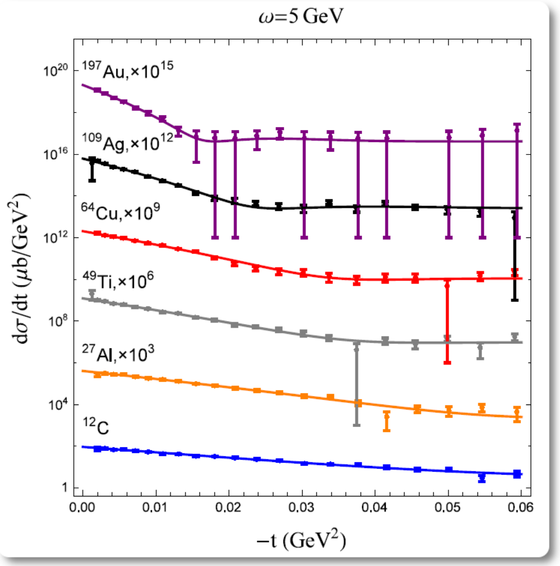

O. Koshchii et al., Phys. Rev. C 103, 064316 (2021)

measurements are available:

- at high energies, E ~ 3–5 GeV
- for the targets ^{4}He, ^{12}C, ^{27}Al, ^{49}Ti, ^{64}Cu, ^{109}Ag, ^{197}Au

problems still existing:

missing data for ^{28}Si, ^{90}Zr, ^{208}Pb + limitation to forward scattering data

Compton slope parameter

feasibility study
to determine the
Compton form factor
with the
high-resolution CATS detector

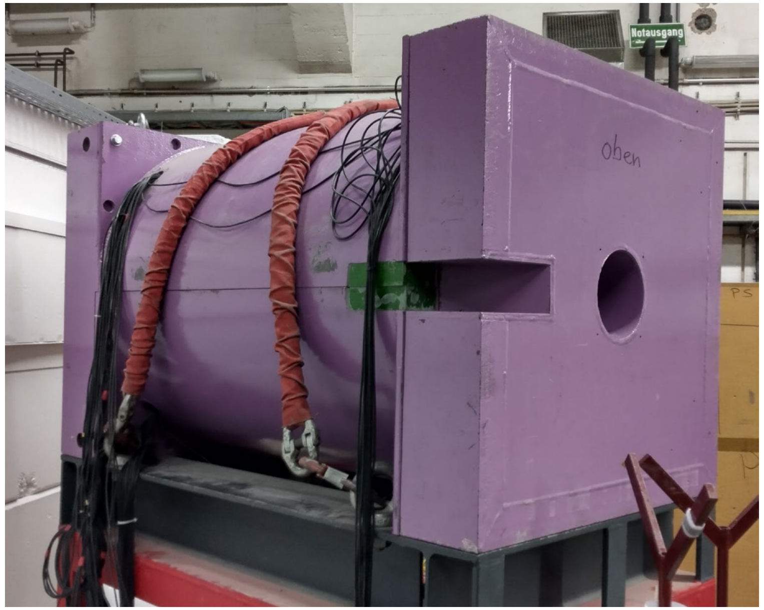

A. Hünger et al., Nucl. Phys. A 620 (1997) 385

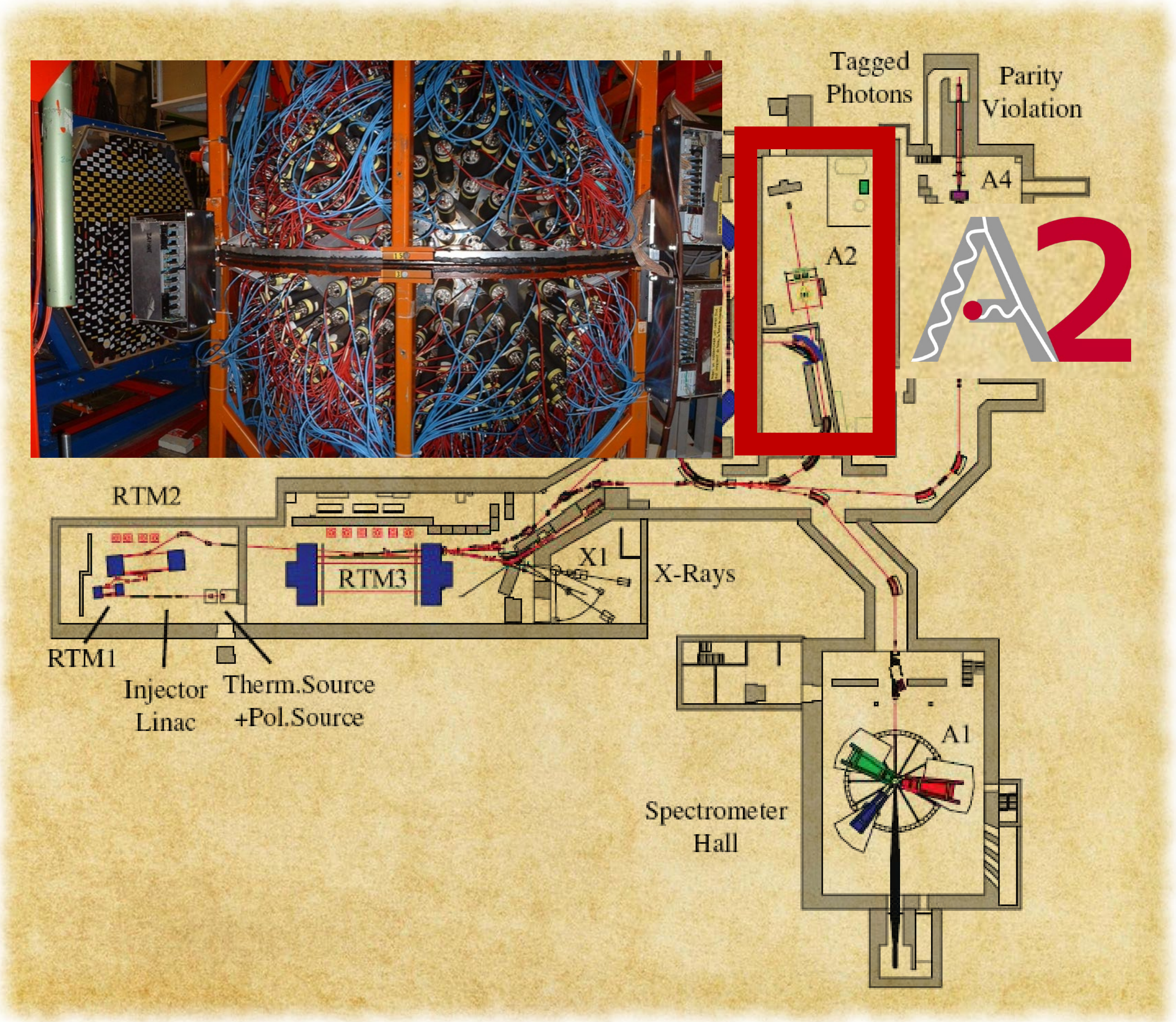

conclusion

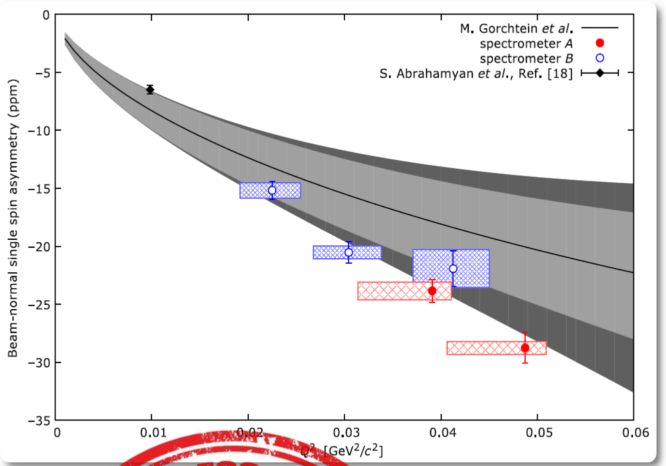

systematic study of transverse asymmetry (^{12}C, ^{28}Si,^{90}Zr)

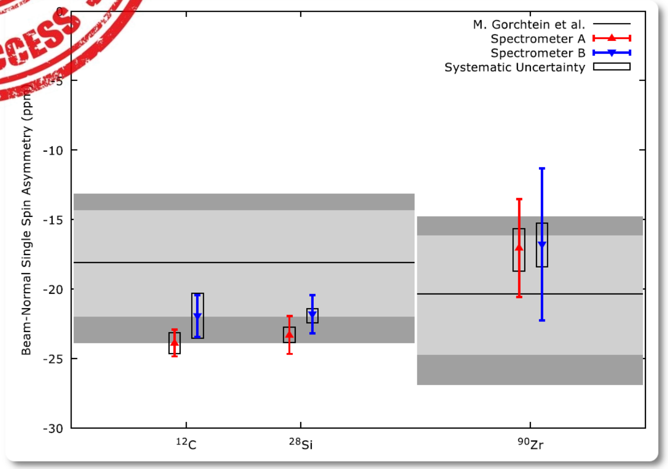

conclusion

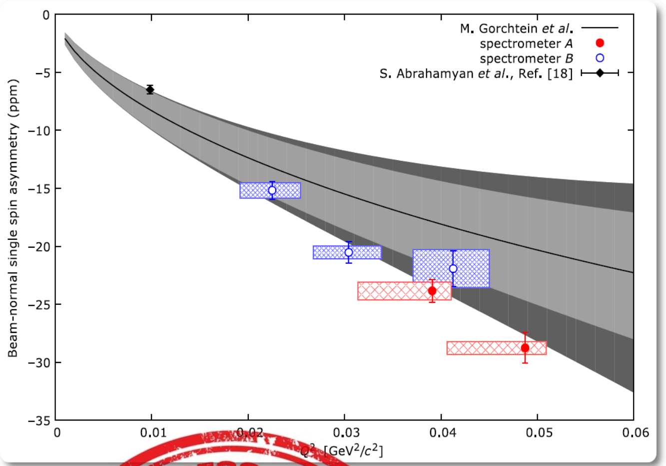

systematic study of transverse asymmetry (^{12}C, ^{28}Si, ^{90}Zr)

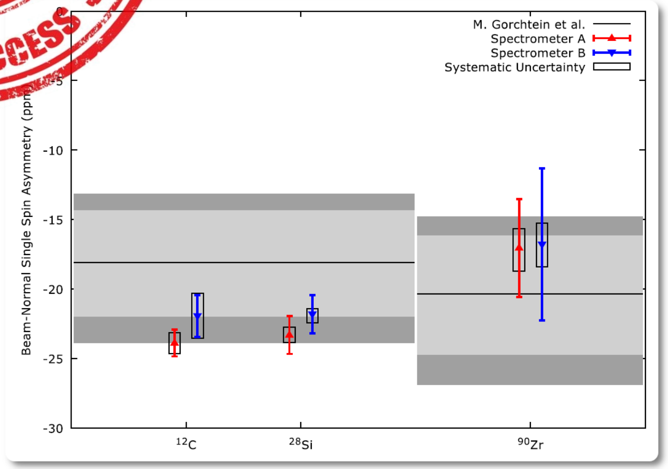

next steps

determine

Compton slope parameter ($\gtrsim$ ^{12}C)

measure

transverse asymmetry ^{208}Pb

on the way to ^{208}Pb

- new electronics system
- proof-of-principle measurement: natural lead